

# Tutorial: Fractional Chern insulators and Exact Diagonalization

Yves H. Kwan<sup>1</sup> and Nicolas Regnault<sup>2,3</sup>

<sup>1</sup>*Princeton Center for Theoretical Science, Princeton University, Princeton, NJ 08544*

<sup>2</sup>*Department of Physics, Princeton University, Princeton, New Jersey 08544, USA*

<sup>3</sup>*Laboratoire de Physique de l'École normale supérieure,*

*ENS, Université PSL, CNRS, Sorbonne Université,*

*Université Paris-Diderot, Sorbonne Paris Cité, 75005 Paris, France*

In this tutorial, we set up a simple exact diagonalization (ED) code to study fractional Chern insulators (FCIs) in a toy Hamiltonian on a kagome lattice model. The basic setup here can be generalized to study more complicated systems, and improved to handle larger Hilbert spaces more efficiently.

## CONTENTS

I. Non-interacting kagome model	2
II. Many-body Hamiltonian and matrix elements	5
III. Exact diagonalization	7
References	10

## I. NON-INTERACTING KAGOME MODEL

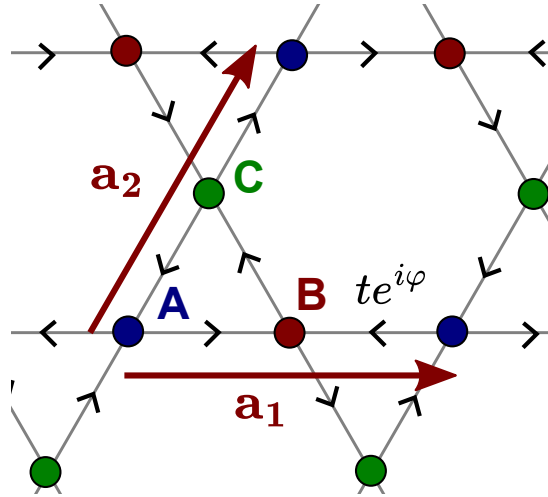


FIG. 1. Kagome lattice model.

For our example of a Chern insulator model, we consider the nearest-neighbour (n.n.) tight-binding model of spinless fermions on the kagome lattice shown in Fig. 1. A similar family of models was introduced in Ref. [1], and studied using exact diagonalization techniques in Refs. [2] and [3]. The unit cell is spanned by two primitive lattice vectors

$$\mathbf{a}_1 = a \begin{pmatrix} 1 \\ 0 \end{pmatrix}, \quad \mathbf{a}_2 = a \begin{pmatrix} 1/2 \\ \sqrt{3}/2 \end{pmatrix} \quad (1)$$

and the corresponding reciprocal lattice vectors are

$$\mathbf{b}_1 = \frac{4\pi}{\sqrt{3}a} \begin{pmatrix} \sqrt{3}/2 \\ -1/2 \end{pmatrix}, \quad \mathbf{b}_2 = \frac{4\pi}{\sqrt{3}a} \begin{pmatrix} 0 \\ 1 \end{pmatrix}, \quad (2)$$

where  $a$  is the lattice constant. The unit cell contains three orbitals (sublattices)  $\alpha = A, B, C$  with corresponding intra-unit-cell coordinates

$$\boldsymbol{\tau}_A = \begin{pmatrix} 0 \\ 0 \end{pmatrix}, \quad \boldsymbol{\tau}_B = \frac{a}{2} \begin{pmatrix} 1 \\ 0 \end{pmatrix}, \quad \boldsymbol{\tau}_C = \frac{a}{2} \begin{pmatrix} 1/2 \\ \sqrt{3}/2 \end{pmatrix}. \quad (3)$$

The non-interacting Hamiltonian  $\hat{H}_0$  consists of n.n. hopping with amplitude  $te^{\pm i\varphi}$ , where the plus sign is taken along the black arrows in Fig. 1. We consider periodic boundary conditions (PBCs) where the system consists of  $N_1$  ( $N_2$ ) unit cells in the  $\mathbf{a}_1$  ( $\mathbf{a}_2$ ) direction. The total number of unit cells is  $N = N_1 N_2$ .

1. Let  $c_{\mathbf{R},\alpha}^\dagger$  be the creation operator for unit cell  $\mathbf{R}$  and orbital  $\alpha$ . We use the Fourier transform convention

$$c_{\mathbf{k},\alpha}^\dagger = \frac{1}{\sqrt{N}} \sum_{\mathbf{R}} e^{i\mathbf{k}\cdot\mathbf{R}} c_{\mathbf{R},\alpha}^\dagger. \quad (4)$$

Show that  $\hat{H}_0$  can be written as

$$\hat{H}_0 = \sum_{\mathbf{k},\alpha,\beta} h_{\alpha\beta}(\mathbf{k}) c_{\mathbf{k},\alpha}^\dagger c_{\mathbf{k},\beta} \quad (5)$$

$$h(\mathbf{k}) = t \begin{pmatrix} 0 & e^{-i\varphi}(1 + e^{-ik_1}) & e^{i\varphi}(1 + e^{-ik_2}) \\ e^{i\varphi}(1 + e^{ik_1}) & 0 & e^{-i\varphi}(1 + e^{i(k_1 - k_2)}) \\ e^{-i\varphi}(1 + e^{ik_2}) & e^{i\varphi}(1 + e^{i(k_2 - k_1)}) & 0 \end{pmatrix}, \quad (6)$$

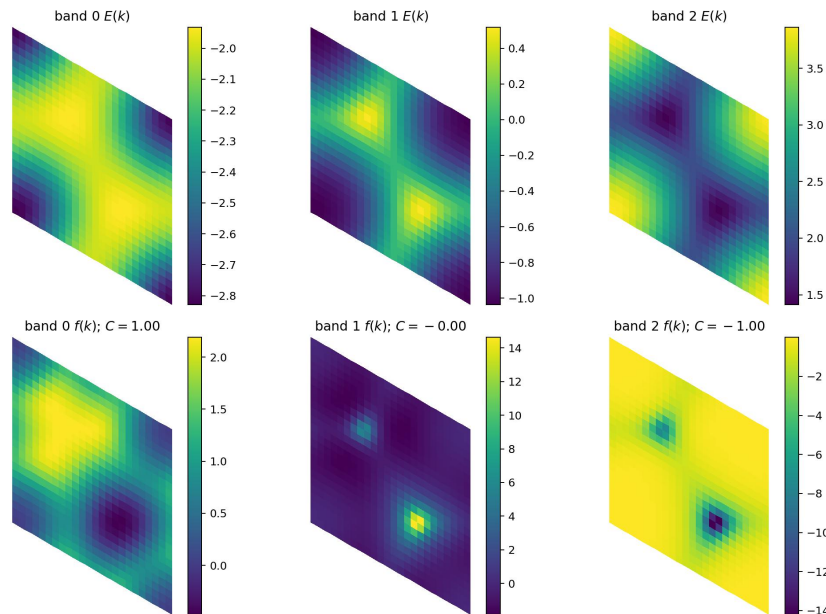


FIG. 2. Kagome tight-binding model for  $t = 1$  and  $\varphi = 5\pi/4$ . Top row: Energy dispersion for each band. The bands are ordered  $n = 0, 1, 2$  in increasing energy. Bottom row: Berry curvature for each band. The Berry curvature  $f(k)$  is normalized here such that e.g. a Chern  $C$  band with uniform curvature would have  $f(k) = C$ . In all plots,  $\mathbf{k} = 0$  corresponds to the corners. Quantities are calculated on a  $N_1 = N_2 = 24$  mesh.

where  $h(\mathbf{k})$  is the Bloch Hamiltonian ( $\alpha = A, B, C$  corresponds to matrix index 0, 1, 2 respectively). Above, we have parameterized the Bloch momentum as

$$\mathbf{k} = \frac{k_1}{2\pi}\mathbf{b}_1 + \frac{k_2}{2\pi}\mathbf{b}_2. \quad (7)$$

[Note that  $h(\mathbf{k})$  does not carry information about the intra-cell coordinates  $\tau_\sigma$ . This can be traced back to our Fourier transform convention in Eq. 4. We'll come back to this point later.]

- From now on, we set  $t = 1$  for simplicity unless otherwise stated. Write a code that generates the dispersion  $\epsilon_n(\mathbf{k})$  and eigenvectors  $u_{n,\alpha}(\mathbf{k})$ , which satisfy

$$\sum_{\beta} h_{\alpha\beta}(\mathbf{k})u_{n,\beta}(\mathbf{k}) = \epsilon_n(\mathbf{k})u_{n,\alpha}(\mathbf{k}), \quad (8)$$

where  $n = 0, 1, 2$  indexes the bands by increasing energy. Plot the dispersion of this Bloch Hamiltonian across the Brillouin zone (BZ) for some values of  $\varphi$ . See the top row of Fig. 2 for example band structures for  $\varphi = 5\pi/4$ . For what values of  $\varphi$  does the model have gapless points?

Consider the case  $\varphi = 0$ . What is the degeneracy of the lowest energy eigenvalue on a periodic system with  $N_1 \times N_2$  unit cells? Can you come up with an argument to explain this degeneracy? See Ref. [4] for hints.

- Recall the expressions for the Berry connection  $\mathbf{A}_n(\mathbf{k})$ , Berry curvature  $F_n(\mathbf{k})$ , and Chern number  $C_n$  for a Bloch band  $n$

$$\mathbf{A}_n(\mathbf{k}) = -i \langle u_n(\mathbf{k}) | \nabla_{\mathbf{k}} | u_n(\mathbf{k}) \rangle \quad (9)$$

$$F_n(\mathbf{k}) = \partial_{k_x} A_{n,y}(\mathbf{k}) - \partial_{k_y} A_{n,x}(\mathbf{k}) \quad (10)$$

$$C_n = \frac{1}{2\pi} \int d^2\mathbf{k} F_n(\mathbf{k}). \quad (11)$$

Why might these formulas be difficult to directly implement in numerical calculations?

4. We can follow Ref. [5] and use a discretized procedure for computing the Berry curvature and Chern number on a momentum grid. In particular for the torus (the system has PBCs so it has the real-space topology of a torus) with dimensions  $N_1 \times N_2$ , the Bloch momenta are

$$\mathbf{k} = \tilde{k}_1 \mathbf{b}_1 / N_1 + \tilde{k}_2 \mathbf{b}_2 / N_2, \quad (12)$$

with  $\tilde{k}_1 = 0, \dots, N_1 - 1$  and  $\tilde{k}_2 = 0, \dots, N_2 - 1$ . Define the link variables (dropping the band index  $n$ )

$$U_\mu(\mathbf{k}) = \frac{\langle u(\mathbf{k}) | u(\mathbf{k} + \mathbf{d}_\mu) \rangle}{|\langle u(\mathbf{k}) | u(\mathbf{k} + \mathbf{d}_\mu) \rangle|}, \quad (13)$$

where  $\mu = 1, 2$ ,  $\mathbf{k}$  is a momentum on the grid, and  $\mathbf{d}_\mu$  is the minimal grid spacing in direction  $\mu$ . The lattice field strength is

$$\tilde{F}(\mathbf{k}) = -i \ln [U_1(\mathbf{k}) U_2(\mathbf{k} + \mathbf{d}_1) U_1(\mathbf{k} + \mathbf{d}_2)^{-1} U_2(\mathbf{k})^{-1}] \quad (14)$$

$$-\pi < \tilde{F}(\mathbf{k}) \leq \pi. \quad (15)$$

For small  $\mathbf{d}_\mu$ , the above expression becomes proportional to the Berry curvature.  $\tilde{F}(\mathbf{k})$  is the Berry phase for going around the plaquette with corners  $\mathbf{k}, \mathbf{k} + \mathbf{d}_2, \mathbf{k} + \mathbf{d}_1 + \mathbf{d}_2, \mathbf{k} + \mathbf{d}_1$ . The discretized Chern number is given by

$$\tilde{C} = \frac{1}{2\pi} \sum_{\mathbf{k}} \tilde{F}(\mathbf{k}). \quad (16)$$

Convince yourself that  $\tilde{F}(\mathbf{k})$  is manifestly gauge-invariant. It can also be shown that  $\tilde{C}$  is quantized to integers. Why is it important that the grid spacing of the momentum mesh is sufficiently fine?

5. Implement the discretized formulas for the kagome model, and plot  $\tilde{C}$  as a function of  $\varphi$  for the three bands. You can check that you have generated  $F_n(\mathbf{k})$  correctly by comparing with the bottom row of Fig. 2 for  $\varphi = 5\pi/4$ . For what values of  $\varphi$  can you find a narrow Chern band with relatively homogeneous Berry curvature?
6. \*\*\* Let's now consider open boundary conditions (OBCs) along one direction, but keeping PBCs along the other direction. For concreteness, let the system be open in the  $\mathbf{a}_1$  direction with  $N_1$  unit cells, and periodic with  $N_2$  unit cells along  $\mathbf{a}_2$ . The Bloch Hamiltonian  $h(k_2)$  is now only diagonal in  $k_2$ . Derive the expression for  $h(k_2)$ . Compute the band structure as a function of  $k_2$  for  $\varphi = 5\pi/4$ . You should find gapless chiral modes that cross the bulk band gaps. Plot the real-space probability density for a state belonging to one of these chiral branches, and discuss its localization along the edge.
7. \*\*\* So far, our momentum meshes have been restricted to the form Eq. 12, with  $N_1$  and  $N_2$  being the only free parameters. One way to generalize this is to consider threading fluxes through the handles of the torus. This is useful for demonstrating the correct spectral flow of eigenvalues. What is the momentum mesh corresponding to fluxes  $\phi_1$  and  $\phi_2$ ?
8. \*\*\* Let's return to the Fourier transform convention for the Bloch basis. Note that Eq. 4 is periodic under  $\mathbf{k} \rightarrow \mathbf{k} + \mathbf{G}$ , where  $\mathbf{G}$  is a reciprocal lattice vector. A periodic gauge is convenient for numerical calculations, where momenta  $\mathbf{k}$  on operators can be 'pulled-back' to the BZ without worrying about additional unitary transformations.

We could consider a different convention

$$\tilde{c}_{\mathbf{k},\alpha}^\dagger = \frac{1}{\sqrt{N}} \sum_{\mathbf{R}} e^{i\mathbf{k} \cdot (\mathbf{R} + \boldsymbol{\tau}_\alpha)} c_{\mathbf{R},\alpha}^\dagger, \quad (17)$$

which accounts for the intra-cell coordinate of the orbitals. How does this sublattice-dependent phase affect the Bloch Hamiltonian? For example, how does the Bloch Hamiltonian in this new convention behave under  $\mathbf{k} \rightarrow \mathbf{k} + \mathbf{G}$ ? Show that the resulting Berry curvature of a given band  $n$  changes, but the Chern number remains invariant. See e.g. Ref. [6] for more discussion of the 'lattice geometry' dependence of certain quantities.

## II. MANY-BODY HAMILTONIAN AND MATRIX ELEMENTS

In this section, we consider the band-projected interacting model for a system of tight-binding fermions. We consider spinless fermions—alternatively we can imagine the spins to be polarized. A lattice model, such as that studied in Sec. I, is characterized by Bravais lattice vectors  $\mathbf{a}_1$  and  $\mathbf{a}_2$ , with corresponding reciprocal lattice vectors  $\mathbf{b}_1$  and  $\mathbf{b}_2$ . A unit cell contains orbitals indexed by  $\alpha$ . We will be interested in systems with PBCs characterized by torus side lengths  $N_1$  and  $N_2$  (in terms of  $\mathbf{a}_1$  and  $\mathbf{a}_2$  respectively), and discrete translation invariance under lattice vectors  $\mathbf{R}$ . A general extended Hubbard-like interaction can be written

$$H_{\text{int}} = \frac{1}{2} \sum_{\mathbf{R}\mathbf{R}'\alpha\beta} V_{\mathbf{R}-\mathbf{R}'}^{\alpha\beta} : n_{\mathbf{R},\alpha} n_{\mathbf{R}',\beta} : \quad (18)$$

where  $n_{\mathbf{R},\alpha} = c_{\mathbf{R},\alpha}^\dagger c_{\mathbf{R},\alpha}$ , and  $: \hat{O} :$  is the normal-ordering operation that brings all creation operators to the left of annihilation operators in  $\hat{O}$ , keeping track of fermionic signs. Note that  $V_{\mathbf{R}}^{\alpha\beta} = V_{-\mathbf{R}}^{\beta\alpha}$ . [The choice of normal-ordering for realistic models of actual materials can be a tricky issue, as e.g. demonstrated by Ref. [7] for rhombohedral pentalayer graphene twisted on hBN—we ignore such problems here.]

1. Using the Fourier transform convention of Eq. 4, show that the interaction Hamiltonian can be expressed in momentum space as

$$H_{\text{int}} = \frac{1}{2N} \sum_{\mathbf{k}_1 \mathbf{k}_2 \mathbf{k}_3 \mathbf{k}_4 \alpha \beta} \tilde{\delta}_{\mathbf{k}_4 = \mathbf{k}_1 + \mathbf{k}_2 - \mathbf{k}_3} V_{\mathbf{k}_1 \mathbf{k}_2 \mathbf{k}_3 \mathbf{k}_4}^{\alpha\beta} c_{\mathbf{k}_1 \alpha}^\dagger c_{\mathbf{k}_2 \beta}^\dagger c_{\mathbf{k}_4 \beta} c_{\mathbf{k}_3 \alpha} \quad (19)$$

$$V_{\mathbf{k}_1 \mathbf{k}_2 \mathbf{k}_3 \mathbf{k}_4}^{\alpha\beta} = \sum_{\mathbf{R}} e^{i(\mathbf{k}_3 - \mathbf{k}_1) \cdot \mathbf{R}} V_{\mathbf{R}}^{\alpha\beta}, \quad (20)$$

where we define a symbol  $\tilde{\delta}_{\mathbf{k}_4 = \mathbf{k}_1 + \mathbf{k}_2 - \mathbf{k}_3}$  that enforces the ‘on-shell’ condition of crystal momentum conservation (i.e.  $\mathbf{k}_1 + \mathbf{k}_2$  should equal  $\mathbf{k}_3 + \mathbf{k}_4$  modulo a reciprocal lattice vector). When on-shell, we have the following identities

$$V_{\mathbf{k}_1 \mathbf{k}_2 \mathbf{k}_3 \mathbf{k}_4}^{\alpha\beta} = V_{\mathbf{k}_2 \mathbf{k}_1 \mathbf{k}_4 \mathbf{k}_3}^{\beta\alpha} = (V_{\mathbf{k}_3 \mathbf{k}_4 \mathbf{k}_1 \mathbf{k}_2}^{\alpha\beta})^*. \quad (21)$$

2. We now want to work in the band basis described by Bloch eigenvectors  $u_{n,\alpha}(\mathbf{k})$  (see Eq. 8) and corresponding creation operators  $d_{\mathbf{k},n}^\dagger$ . Express the interaction Hamiltonian in the band basis.
3. In the following, we will be interested in projecting the Hamiltonian into some specific band  $n$ . Doing so will significantly reduce the many-body Hilbert space dimension and the computational difficulty. If there are sizable single-particle gaps separating the band of interest from other bands, then such projection may be physically justified. For some situations, it may not be justified at all!

Operationally, we interpret projection as simply restricting the band indices to band  $n$  for the purposes of this tutorial. [This implicitly makes an assumption about the role of the other bands]. Show that the interaction Hamiltonian is

$$H_{\text{int}} = \frac{1}{2N} \sum_{\mathbf{k}_1 \mathbf{k}_2 \mathbf{k}_3 \mathbf{k}_4} \tilde{\delta}_{\mathbf{k}_4 = \mathbf{k}_1 + \mathbf{k}_2 - \mathbf{k}_3} U_{\mathbf{k}_1 \mathbf{k}_2 \mathbf{k}_3 \mathbf{k}_4} d_{\mathbf{k}_1}^\dagger d_{\mathbf{k}_2}^\dagger d_{\mathbf{k}_4} d_{\mathbf{k}_3} \quad (22)$$

$$U_{\mathbf{k}_1 \mathbf{k}_2 \mathbf{k}_3 \mathbf{k}_4} = \sum_{\alpha\beta} u_\alpha^*(\mathbf{k}_1) u_\beta^*(\mathbf{k}_2) u_\alpha(\mathbf{k}_3) u_\beta(\mathbf{k}_4) V_{\mathbf{k}_1 \mathbf{k}_2 \mathbf{k}_3 \mathbf{k}_4}^{\alpha\beta} \quad (23)$$

where we have hidden the band index  $n$  above. When on-shell, we have the relations

$$U_{\mathbf{k}_1 \mathbf{k}_2 \mathbf{k}_3 \mathbf{k}_4} = U_{\mathbf{k}_2 \mathbf{k}_1 \mathbf{k}_4 \mathbf{k}_3} = (U_{\mathbf{k}_3 \mathbf{k}_4 \mathbf{k}_1 \mathbf{k}_2})^*. \quad (24)$$

Write some code that generates  $U_{\mathbf{k}_1 \mathbf{k}_2 \mathbf{k}_3 \mathbf{k}_4}$  for the kagome model (see Sec. I) with n.n. Hubbard interactions of strength  $V$ , i.e.  $V_{\mathbf{R}-\mathbf{R}'}^{\alpha\beta} = V$  in Eq. 18 if sites  $(\mathbf{R}, \alpha)$  and  $(\mathbf{R}', \beta)$  are nearest neighbours. Verifying Eq. 24 provides a quick check for any bugs in the code.

To check that your code is working fine, we provide sample matrix elements  $U_{\mathbf{k}_1 \mathbf{k}_2 \mathbf{k}_3 \mathbf{k}_4}$  in the text files `Uint_N_3_4.txt`, `Uint_N_3_5.txt` and `Uint_N_4_4.txt` for  $(N_1, N_2) = (3, 4), (3, 5), (4, 4)$  respectively. These

correspond to  $V = 1$  and projection onto the lowest ( $n = 0$ ) band of the Kagome model with  $t = 1, \varphi = 5\pi/4$ . Each row in the text files corresponds to  $[\tilde{k}_{1,1}, \tilde{k}_{1,2}, \tilde{k}_{2,1}, \tilde{k}_{2,2}, \tilde{k}_{3,1}, \tilde{k}_{3,2}, \text{Re}U_{\mathbf{k}_1\mathbf{k}_2\mathbf{k}_3\mathbf{k}_4}, \text{Im}U_{\mathbf{k}_1\mathbf{k}_2\mathbf{k}_3\mathbf{k}_4}]$ . We use the momentum labelling convention of Eq. 12, so that e.g.  $\mathbf{k}_1 = \tilde{k}_{1,1}\mathbf{b}_1/N_1 + \tilde{k}_{1,2}\mathbf{b}_2/N_2$ , etc. The momentum  $\mathbf{k}_4$  is not explicitly mentioned because it is fixed by momentum conservation.

### III. EXACT DIAGONALIZATION

In this section, we discuss some details of how to implement a basic ED code. Note that the priority here is to gain some understanding of the challenges involved, and to get a working code up and running. Hence, the code written here will by no means be particularly efficient! The code examples and data will be given in Python, but feel free to use other programming languages. We will assume a one-band projected Hamiltonian (see Sec. II) on a lattice with  $N = N_1 \times N_2$  unit cells, and work directly in momentum space (why?).

1. The main limitation of ED is the rapid growth of the Hilbert space as the system size increases. For a system of  $N$  unit cells, what is the total many-body Hilbert space dimension? What is the maximum size of  $N$  for which you could store the full many-body wavefunction on your computer?

Clearly, it is imperative to cut down the effective Hilbert space dimension, which would reduce the memory requirements and the time needed for matrix diagonalization. This can be achieved by considering the symmetries of the problem, which will block-diagonalize the many-body Hamiltonian. Then, each block can be diagonalized separately (and perhaps only a subset of the symmetry sectors are required). The simplest symmetry to incorporate is the  $U_c(1)$  symmetry corresponding to electron number conservation. What is the many-body Hilbert space dimension for the sector with  $N_e$  electrons? For  $N = 15$  and  $N_e = 6$ , you should find a Hilbert space dimension of 5005.

Consider a filling factor of  $\nu = N_e/N = 1/3$ . What is the maximum system size for which you could store the many-body wavefunction on your computer? If there are other internal symmetries, then these could be exploited as well. For instance if there is a spin degree of freedom and  $S_z$  conservation, then the symmetry sectors can be labelled  $(N_e, S_z)$ .

The systems of interest here also satisfy a discrete translation invariance, such that the Hamiltonian decomposes into  $N = N_1 \times N_2$  many-body momentum sectors labelled by  $\mathbf{K}_{\text{tot}}$ . Eq. 12. In this case, there is no analytical formula for the Hilbert space dimension of a given  $(N_e, \mathbf{K}_{\text{tot}})$ , but can you come up with an approximate estimate? Write some code that exactly computes the dimension for a given  $(N_e, \mathbf{K}_{\text{tot}})$ . For  $N_1 = 3, N_2 = 5$  and  $N_e = 6$ , you should find a Hilbert space dimension  $\mathcal{D} = 335$  for  $\mathbf{K}_{\text{tot}} = (0, 0)$  and  $\mathcal{D} = 333$  for  $\mathbf{K}_{\text{tot}} = (1, 4)$ . Note that rotational symmetries and other point group symmetries could be exploited to further cut down the Hilbert space, but this is beyond the scope of this tutorial.

2. Let's now prepare for ED by specifying the many-body basis in more detail. We build the basis by considering Fock states where each single-particle orbital (which is uniquely labelled by  $\mathbf{k}$  in our one-band problem) is either occupied or unoccupied. Hence, each basis state is uniquely specified by the occupation numbers  $n_{\mathbf{k}} = 0, 1$ .

We need to worry about two more things: 1) a convenient representation of each basis state for the numerics; 2) a canonical ordering of operators to account for the fermionic sign (we are dealing with electrons here). It will be convenient to label momenta using the quasi-1D parameterization  $K$  defined by

$$K = \tilde{k}_2 + N_2 \tilde{k}_1 \tag{25}$$

$$\mathbf{k} = \tilde{k}_1 \mathbf{b}_1 / N_1 + \tilde{k}_2 \mathbf{b}_2 / N_2, \tag{26}$$

with  $\tilde{k}_1 = 0, \dots, N_1 - 1$  and  $\tilde{k}_2 = 0, \dots, N_2 - 1$ . So  $K$  runs from  $0, \dots, N - 1$ .

Choose a canonical ordering of single-particle orbitals for specifying the basis Fock states. One convention is to order the creation operators so that lower values of  $K$  are placed to the left, such that a generic Fock basis state (with  $N_e$  particles) would be

$$d_{K_0}^\dagger d_{K_1}^\dagger \dots d_{K_{N_e-1}}^\dagger |\text{vac}\rangle \text{ with } K_0 < K_1 < \dots < K_{N_e-1}. \tag{27}$$

There are several ways to represent a given Fock basis state in the code, depending on the programming language and requirement for efficiency. In the Python example, we directly encode using ordered tuples  $(K_0, K_1, \dots)$  for simplicity. But it is most common to represent a Fock state using an integer

$$x[n_K] = \sum_0^{N-1} n_K \times 2^K \tag{28}$$

which is amenable to various numerical tricks for performing certain operations—see e.g. Ref. [8]. In a binary representation, the  $n_K$  directly appear as 0's and 1's in the bitstring.

Whichever representation you use, you should be comfortable performing the following operations in your code:

- For a given representation (e.g. an integer if using Eq. 28) of some Fock state, determine its particle number  $N_e$  and total momentum  $\mathbf{K}_{\text{tot}}$ .
  - From some initial Fock basis state, find the representation of the final state (if any) obtained by acting with  $d_{\mathbf{k}}^\dagger$  or  $d_{\mathbf{k}}$ , including the fermionic sign.
3. Write some code that generates the basis list corresponding to a fixed  $(N_e, \mathbf{K}_{\text{tot}})$ . Let the dimension of the Hilbert subspace be  $\mathcal{D}_{N_e, \mathbf{K}_{\text{tot}}}$ . Each basis state should be assigned a unique index in  $0, \dots, \mathcal{D}_{N_e, \mathbf{K}_{\text{tot}}} - 1$  for the purposes of building the Hamiltonian in the next step. Also write a routine that returns, starting from an initial Fock state, the final Fock state, its unique index, and the fermionic sign from acting with a  $\mathbf{K}_{\text{tot}}$ -conserving operator  $d_{\mathbf{k}_0}^\dagger d_{\mathbf{k}_1}^\dagger d_{\mathbf{k}_3} d_{\mathbf{k}_2}$  (i.e.  $\mathbf{k}_3 = \mathbf{k}_0 + \mathbf{k}_1 - \mathbf{k}_2$  modulo a reciprocal lattice vector). Check that the final state in the code always maintains the same particle number  $N_e$  and total momentum  $\mathbf{K}_{\text{tot}}$ .
  4. We are now ready to build the Hamiltonian. Let's review the projected Hamiltonian. The total interacting Hamiltonian that we will study is

$$H_{\text{tot}} = \kappa H_0 + H_{\text{int}} \quad (29)$$

$$H_0 = \sum_{\mathbf{k}} \epsilon(\mathbf{k}) d_{\mathbf{k}}^\dagger d_{\mathbf{k}} \quad (30)$$

$$H_{\text{int}} = \frac{1}{2N} \sum_{\mathbf{k}_1 \mathbf{k}_2 \mathbf{k}_3 \mathbf{k}_4} \tilde{\delta}_{\mathbf{k}_4 = \mathbf{k}_1 + \mathbf{k}_2 - \mathbf{k}_3} U_{\mathbf{k}_1 \mathbf{k}_2 \mathbf{k}_3 \mathbf{k}_4} d_{\mathbf{k}_1}^\dagger d_{\mathbf{k}_2}^\dagger d_{\mathbf{k}_4} d_{\mathbf{k}_3} \quad (31)$$

where  $H_0$  is the single-particle dispersion and  $H_{\text{int}}$  is the interaction taken from Eq. 22, where the matrix elements satisfy Eq. 24. Recall that the symbol  $\tilde{\delta}_{\mathbf{k}_4 = \mathbf{k}_1 + \mathbf{k}_2 - \mathbf{k}_3}$  enforces the ‘on-shell’ condition of crystal momentum conservation (i.e.  $\mathbf{k}_1 + \mathbf{k}_2$  should equal  $\mathbf{k}_3 + \mathbf{k}_4$  modulo a reciprocal lattice vector). We have introduced an artificial ‘band-flattening’ parameter  $\kappa$  to control the bandwidth. It is common in many FCI studies of model Hamiltonians to work with  $\kappa = 0$  which mimics the flat dispersion of a Landau level.

As a warm-up, write some code that generates  $H_0$  in some given  $(N_e, K_{\text{tot}})$  sector, given some input band dispersion  $\epsilon(\mathbf{k})$ . For simplicity in this tutorial, you can store the entire matrix as a dense  $\mathcal{D}_{N_e, K_{\text{tot}}} \times \mathcal{D}_{N_e, K_{\text{tot}}}$  matrix, since the Hilbert subspaces we consider here are small enough to perform full diagonalization. For larger Hilbert spaces, one would resort to sparse matrix techniques such as the Lanczos algorithm. In this case, one would use a sparse matrix data format, or forgo storing the Hamiltonian all together in some situations.

5. We now turn to the interaction Hamiltonian  $H_{\text{int}}$  (Eq. 31). Write some code to construct the matrix representation of  $H_{\text{int}}$  in some  $(N_e, K_{\text{tot}})$  sector, given a set of matrix elements  $U_{\mathbf{k}_1 \mathbf{k}_2 \mathbf{k}_3 \mathbf{k}_4}$ . The  $U_{\mathbf{k}_1 \mathbf{k}_2 \mathbf{k}_3 \mathbf{k}_4}$  could be e.g. read in from a formatted text file. Either generate the matrix elements yourself, or use the reference matrix elements described at the end of Sec. II. When populating the entries of  $H_{\text{int}}$ , ensure that you account for any fermionic signs. Convince yourself that the interaction Hamiltonian becomes sparser as the system size increases for a fixed filling  $\nu = N_e/N$ . As an intermediate check, you should find that for  $N_1 = 3, N_2 = 5, N_e = 5, \mathbf{K}_{\text{tot}} = (0, 0)$ ,  $H_{\text{int}}$  is a  $201 \times 201$  matrix with 7251 non-zero entries.

At the moment, there are multiple terms in Eq. 31 that could connect a given pair of many-body Fock states. You may find it useful when generating the interaction Hamiltonian matrix to first recast the sum as over ordered ‘creation pairs’  $\mathbf{k}_1 < \mathbf{k}_2$  and ordered ‘annihilation pairs’  $\mathbf{k}_3 < \mathbf{k}_4$ , where some ordering  $<$  on Bloch momenta has been chosen (e.g. the canonical ordering when defining the Fock basis states using the linearized momentum of Eq. 25). Show that we can then write

$$H_{\text{int}} = \frac{1}{N} \sum_{\mathbf{k}_1 \mathbf{k}_2 \mathbf{k}_3 \mathbf{k}_4 \text{ s.t. } \mathbf{k}_1 < \mathbf{k}_2 \text{ and } \mathbf{k}_3 < \mathbf{k}_4} \tilde{\delta}_{\mathbf{k}_4 = \mathbf{k}_1 + \mathbf{k}_2 - \mathbf{k}_3} \tilde{U}_{\mathbf{k}_1 \mathbf{k}_2 \mathbf{k}_3 \mathbf{k}_4} d_{\mathbf{k}_1}^\dagger d_{\mathbf{k}_2}^\dagger d_{\mathbf{k}_4} d_{\mathbf{k}_3} \quad (32)$$

$$\tilde{U}_{\mathbf{k}_1 \mathbf{k}_2 \mathbf{k}_3 \mathbf{k}_4} = U_{\mathbf{k}_1 \mathbf{k}_2 \mathbf{k}_3 \mathbf{k}_4} - U_{\mathbf{k}_1 \mathbf{k}_2 \mathbf{k}_4 \mathbf{k}_3} = \tilde{U}_{\mathbf{k}_2 \mathbf{k}_1 \mathbf{k}_4 \mathbf{k}_3} = -\tilde{U}_{\mathbf{k}_1 \mathbf{k}_2 \mathbf{k}_4 \mathbf{k}_3} = (\tilde{U}_{\mathbf{k}_3 \mathbf{k}_4 \mathbf{k}_1 \mathbf{k}_2})^*. \quad (33)$$

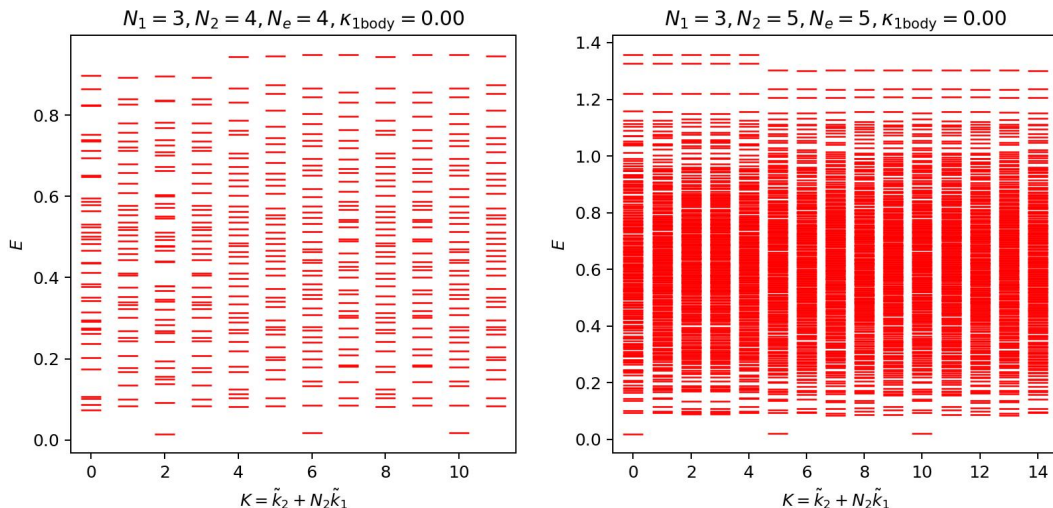


FIG. 3. Full momentum-resolved ED spectrum for the Kagome tight-binding model with  $t = 1, \varphi = 5\pi/4$  and n.n. Hubbard interactions of strength  $V = 1$  projected onto the lowest band. We use the band-flattened limit  $\kappa = 0$ . Left:  $N_1 = 3, N_2 = 4, N_e = 4$ . Right:  $N_1 = 3, N_2 = 5, N_e = 5$ .

6. For the kagome model described in Secs. I and II, generate the many-body spectrum across all momentum sectors for  $N_e = 4$  electrons, system size  $N_1 = 3, N_2 = 4$ , kagome hopping phase  $\varphi = 5\pi/4$ , and n.n. interaction strength  $V = 1$ . Project to band  $n = 0$  (the lowest band) using band index restriction (i.e. ignore any possible effects from the other bands), and work in the flattened limit  $\kappa = 0$ . Do the same for  $N_1 = 3, N_2 = 5, N_e = 5$ . Plot the full momentum-resolved many-body spectrum, and compare with Fig. 3. What features do you notice about the entire spectrum?
7. In the previous exercise, we computed the many-body spectrum for  $\nu = 1/3$  filling of a flat Chern band. Do we have an FCI ground state, in particular the FCI analog of a  $1/3$  Laughlin state? How can we tell? The simplest signature of an FCI is its topological degeneracy on a torus. Our calculation is on a torus since we use periodic boundary conditions in both directions. Therefore, we expect three quasi-degenerate ground states, separated from higher states by a gap. As the system size  $N$  increases, the splitting between the three quasi-degenerate ground states should exponentially decrease, and the gap  $\Delta_3$  to excited states should converge to a finite value. Define the ‘spread’  $\delta_3$  as the bandwidth of the lowest three states (across all momentum sectors). Compute the FCI spread/gap ratio  $\delta_3/\Delta_3$  for your ED spectra.
8. We can do better and use the momentum-resolved information. In particular, we are interested in the momentum-dependent quasi-degeneracy  $\mathcal{N}^{\text{FCI}}(k_1, k_2)$  of ground states in the many-body momentum sector  $(k_1, k_2)$ . There is a procedure for determining  $\mathcal{N}^{\text{FCI}}(k_1, k_2)$  from the degeneracy  $\mathcal{N}^{\text{FQH}}(k'_1, k'_2)$  of the analogous fractional quantum Hall state on the torus with  $N = N_1 \times N_2$  fluxes. The formula is (see e.g. Ref. [9])

$$\mathcal{N}^{\text{FCI}}(k_1, k_2) = \sum_{k'_1, k'_2=0}^{N_e-1} \frac{M_1 M_2}{M_0} \mathcal{N}^{\text{FQH}}(k'_1, k'_2) \delta_{k'_1 \bmod M_1, k_1 \bmod M_1} \delta_{k'_2 \bmod M_2, k_2 \bmod M_2} \quad (34)$$

$$M_1 = \text{GCD}(N_e, N_1), \quad M_2 = \text{GCD}(N_e, N_2), \quad M_0 = \text{GCD}(N_e, N). \quad (35)$$

For the  $\nu = 1/3$  Laughlin state with  $N = 12$  fluxes, you will need to use  $\mathcal{N}^{\text{FQH}}(2, 2) = 1$  (the other values are zero for  $k'_1, k'_2 < N_e$ ). What are the ground state momenta for the  $\nu = 1/3$  FCI lattice for the  $3 \times 4$  lattice? Do the same for the  $\nu = 1/3$  FCI on the  $3 \times 5$  lattice, where you need to use  $\mathcal{N}^{\text{FQH}}(0, 0) = 1$ . Are these consistent with your ED spectra? The definition of the FCI spread  $\delta_3$  should be refined to account for the expected many-body momenta of the putative topological quasi-degenerate ground states.

We should be careful about other (less exotic) phases that could also manifest the same momentum-resolved quasi-degeneracy. The system sizes we have studied are all a multiple of 3 in one direction. Consider a charge density wave (CDW) at  $\nu = 1/3$  that triples the unit cell along this direction. What would be the expected ground state momenta of such a CDW? Could such a CDW be distinguished from an FCI solely on

the basis of the momentum-resolved quasi-degeneracy? See e.g. Ref. [10] for more discussion on diagnosing spontaneous symmetry-breaking in ED, including continuous symmetries.

9. We can study the properties of the ground states directly to obtain more evidence in favor of an FCI state. One easy-to-implement diagnostic is the average occupation  $\langle n_{\mathbf{k}} \rangle$  for a many-body wavefunction. Write some code that computes this quantity, averaged over the three quasi-degenerate states. We expect this to be uniform and close to  $1/3$  across the BZ for an FCI. On the other hand, a CDW is expected to have a strongly fluctuating  $\langle n_{\mathbf{k}} \rangle$ .

For the  $N_1 = 3, N_2 = 5, N_e = 5$  calculation, you should find the following average of  $\langle n_{\mathbf{k}} \rangle$  over the three quasi-degenerate states:

[0.38646021 0.34280379 0.31814227 0.31814227 0.34280379 0.3238678 0.33192043 0.32271955  
0.3365834 0.33073265 0.3238678 0.33073265 0.3365834 0.32271955 0.33192043].

10. A striking feature of FCIs and fractional quantum Hall states is the fractional charge and statistics of their quasiparticle excitations. Compute the ED spectrum across all momentum sectors for  $N_1 = 4, N_2 = 4, N_e = 5$ . How many quasiholes of the  $\nu = 1/3$  state does this correspond to? The spectrum should clearly separate into a low-lying manifold of quasihole excitations, and higher energy non-universal states.

Count the number of low-lying states for each  $\mathbf{K}_{\text{tot}}$ . The mapping from FQH to FCI states leads to the prediction that there is one low-lying state per  $\mathbf{K}_{\text{tot}}$ . Does this match your numerical results?

- 
- [1] E. Tang, J.-W. Mei, and X.-G. Wen, High-temperature fractional quantum hall states, *Phys. Rev. Lett.* **106**, 236802 (2011).  
 [2] Y.-L. Wu, B. A. Bernevig, and N. Regnault, Zoology of fractional chern insulators, *Phys. Rev. B* **85**, 075116 (2012).  
 [3] C. Repellin, B. A. Bernevig, and N. Regnault,  $z_2$  fractional topological insulators in two dimensions, *Phys. Rev. B* **90**, 245401 (2014).  
 [4] D. L. Bergman, C. Wu, and L. Balents, Band touching from real-space topology in frustrated hopping models, *Phys. Rev. B* **78**, 125104 (2008).  
 [5] T. Fukui, Y. Hatsugai, and H. Suzuki, Chern numbers in discretized brillouin zone: efficient method of computing (spin) hall conductances, *Journal of the Physical Society of Japan* **74**, 1674 (2005).  
 [6] S. H. Simon and M. S. Rudner, Contrasting lattice geometry dependent versus independent quantities: Ramifications for berry curvature, energy gaps, and dynamics, *Phys. Rev. B* **102**, 165148 (2020).  
 [7] Y. H. Kwan, J. Yu, J. Herzog-Arbeitman, D. K. Efetov, N. Regnault, and B. A. Bernevig, *Moiré fractional chern insulators iii: Hartree-fock phase diagram, magic angle regime for chern insulator states, the role of the moiré potential and goldstone gaps in rhombohedral graphene superlattices* (2023), arXiv:2312.11617 [cond-mat.str-el].  
 [8] <https://graphics.stanford.edu/~seander/bithacks.html>.  
 [9] T. Liu, C. Repellin, B. A. Bernevig, and N. Regnault, Fractional chern insulators beyond laughlin states, *Phys. Rev. B* **87**, 205136 (2013).  
 [10] A. Wietek, M. Schuler, and A. M. Läuchli, *Studying continuous symmetry breaking using energy level spectroscopy* (2017), arXiv:1704.08622 [cond-mat.str-el].